*J Mater Sci* (2017) 52:6581–6590

# Preparation and photothermal study of polystyrene coated with gold nanoshell composite particles

Hepeng Zhang[1,*], Yonggang Zhang[1], Chen Wu[1], Haochen Tan[1], Shenqiang Wang[1], Baoliang Zhang[1], and Qiuyu Zhang[1]

[1] *The Key Laboratory of Space Applied Physics and Chemistry, School of Science, Northwestern Polytechnical University, Xi'an 710072, China*

**Received:** 26 October 2016
**Accepted:** 3 February 2017
**Published online:** 13 February 2017



## ABSTRACT

Polystyrene coated with gold nanoshell composite particles, with good photothermal properties, were prepared by electrostatic self-assembly. Firstly, polystyrene (PS) microspheres were synthesized by emulsifier-free emulsion polymerization, and it is determined that the PS microsphere has an average diameter of 165 nm, carboxyl on the surface, and its surface potential turned into +38.3 mV after modified by polyallylamine hydrochloride (PAH). Secondly, gold seeds, with an average diameter of 5.14 nm and surface potential of −10.7 mV, were prepared via sodium borohydride reducing chloroauric acid. Then, gold seeds were adsorbed on the surface of PS microspheres by electrostatic self-assembly and the composite particles were obtained after gold seeds grew multiple times. Finally, 0.3 mg/mL composite particles dispersion was irradiated with a near-infrared (NIR) light source and the temperature of the dispersion increased 13 °C after 5 min.

## Introduction

In recent years, cancer has become one of the major diseases that threaten human health. The latest data show that another 4.292 million people were diagnosed with cancer and 2.814 million people with cancer died in 2015. Currently, the main methods to treat cancer are surgery, chemotherapy and radiotherapy. However, surgical treatment has some problems of uncomplete cancerous tissues and cells remove and possible recurrence. Due to the lack of specific selectivity, chemotherapy and radiotherapy can cause destruction to normal cells as well as cancer cells, which damages the human body greatly [1].

The novel nanomaterials with optical and magnetic features provide an effective platform for fighting against cancer, on which thermotherapy, a new kind of cancer treatments, is developed [2–6]. The basic mechanism of thermotherapy is that cancer cells are more sensitive to heat than normal cells and can be easily killed and destroyed at high temperature. Compared with the above-mentioned treatments, thermotherapy has more advantages such as stronger specificity to cancer cells and less toxic side effect [1].

Address correspondence to E-mail: zhanghepeng@nwpu.edu.cn

DOI 10.1007/s10853-017-0893-0

Besides, nanoparticles can be endowed with functions of thermotherapy, chemotherapy, photodynamic therapy and drug delivery by structural design and optimization. Photothermal particles are the core and focus on the field of thermotherapy research [7–14].

Photothermal therapy (PTT) is a method that certain nanoparticles can absorb NIR with good permeability to biological organs and generate heat to kill cancer cells via surface plasmon resonance. Gold nanoparticles, nanorods and nanoshells [11, 15–22], carbon nanomaterials [23–29] and CuS/Se [30, 31] are common photothermal particles. At present, scientists have been constantly exploring new photothermal particles. We prepared PS microspheres by emulsifier-free emulsion polymerization in this article. On this basis, gold seeds were adsorbed on the surface of these microspheres by electrostatic adsorption. Finally, novel photothermal composite particles with core–shell structure, polystyrene coated with gold nanoshell (named as PS@Au), were obtained via gold seeds growth and the photothermal properties were characterized.

## Experimental section

### Materials

Styrene (St, TCRY) and acrylic acid (AA, TCRY) were used after being distilled in vacuum. Potassium persulfate (KPS), polyallylamine hydrochloride (PAH), sodium borohydride ($NaBH_4$), chloroauric acid ($HAuCl_4$) and other chemicals, purchased from Sinopharm Chemical Reagent Co., Ltd, were directly used without any treatment.

### Preparation of gold seeds

37.5 mg $NaBH_4$ was dissolved in 50 mL 10 g/L trisodium citrate aqueous solution, and 2.5 mL 10 g/L $HAuCl_4$ aqueous solution was diluted with water to 250 mL. After magnetic stirring for 5 min, 2.5 mL 10 g/L trisodium citrate aqueous solution was added to the above solution. One minute later, 2.5 mL $NaBH_4$ solution prepared above was added to the mixture, and after reacting for 5 min the products were stored at 4 °C for later use [32–34].

### Preparation of PS microspheres

PS microspheres were prepared by emulsifier-free emulsion polymerization. A typical preparation process is as follows: 2.56 g St and 0.44 g AA were dissolved in 80 mL water and the mixture was added to a 250-mL three-necked flask. 0.07 g KPS was dissolved in 20 mL water to be added to the solution in the flask. And then the emulsion in the flask would react at 80 °C for 8 h with a stirring rate of 200 rpm. After cooling to room temperature, the products were stored for later use.

### Surface modification of PS microspheres

Ten milliliters (solid content was 2 mg/mL) PS microspheres emulsion was added to 100 mL PAH aqueous solution with different concentration (1.5, 3, 4.5 g/L), respectively. After magnetic stirring for 30 min, the mixture was centrifuged for 20 min at a rotational speed of 9000 rpm, then the supernatant was removed and distilled water was added to clean the products by ultrasonic. The above steps were repeated twice to remove the PAH not adsorbing on the surface of PS microspheres. Finally, the centrifuged sample was dispersed in water for later use.

### Preparation of PS@Au composite particles

#### *Adsorption of gold seeds on the surface of PS microspheres*

PS microspheres prepared above were diluted to 50 mL with water, gold seeds aqueous solution was added, and the solution would react for 30 min with magnetic stirring. Then, the obtained solution was centrifuged for 15 min at a rotational speed of 10000 rpm, the supernatant was removed, and the particles were dispersed into water by ultrasonic. The centrifugal process was repeated, and the products were dispersed in water for later use (dispersion 1).

#### *Secondary growth of gold seeds on the surface of PS microspheres*

3.5 mL $HAuCl_4$ (aq.) and 13 mL trisodium citrate (aq.) were added to 223.5 mL water-diluted dispersion 1 (55 mL). After magnetic stirring for 5 min, a certain amount of $NH_2OH{\cdot}HCl$ (aq.) was added to the mixture and the reaction was kept for 30 min.

**Table 1** Average diameter of as-prepared gold seeds with different concentrations of $HAuCl_4$

| No | Concentration of $HAuCl_4$ (g/L) | Average diameter of gold seeds (nm) |
|---|---|---|
| 1 | 0.1 | 5.14 |
| 2 | 0.2 | 8.23 |
| 3 | 0.5 | 24.37 |

*Multiple-growth of gold seeds on the surface of PS microspheres*

The growth of gold seeds on the surface of PS microspheres was repeated until gold seeds grew big enough to form composite particles with dense gold nanoshells.

## Characterization

The diameter and distribution of PS microspheres were measured using America Beckman Coulter LS13320 laser particle size analyzer. Surface Zeta potential of particles was measured by US Malvern company Zetasizer ZEN 3500 light-scattering spectrometer. Morphology of particles was characterized by Tecnai $G^2$ F20 S-TWIN field emission transmission electron microscope of America FEI Company. Surface morphology of samples and energy-dispersive spectroscopy (EDS) were characterized by America FEI Quanta 400 FEG environmental scanning electron microscope. X-ray diffraction (XRD) patterns were tested by X-ray powder diffraction (XRD-7000S from Shimadzu) to characterize the gold on the surface of PS@Au composite particles. The NIR absorbance of the samples was analyzed using a UV–Vis spectrophotometer (BlueStar, LabTech). Photothermal effect was characterized by gauging the variation of temperature by changing the radiation time, using platinum and rhodium probe as the temperature sensor, when the 0.3 mg/mL composite particles dispersion was irradiated with a NIR light source with a center wavelength of 808 nm and output power of 0.97 W.

# Results and discussion

## Properties of gold seeds

In order to realize gold seeds coating on the surface of organic microspheres uniformly, the diameter of gold seeds should be as small as possible. However, in the process of preparing gold seeds via sodium borohydride reducing chloroauric acid, chloroauric acid concentration has a crucial impact on the diameter of gold seeds. Therefore, the proportion of chloroauric acid and sodium borohydride was kept invariable, several different concentrations of chloroauric acid were chosen to prepare gold seeds, and the influence of the concentration of the chloroauric acid on the diameter of the as-prepared gold seeds was investigated.

Table 1 shows the particle size of as-prepared gold seeds The data in Table 1 show that the diameter of as-prepared gold seeds increases dramatically as the concentration of chloroauric acid increases, which is mainly caused by crystal nucleus growing faster in high chloroauric acid concentration system after the homogeneous nucleation. When the concentration of chloroauric acid is 0.1 g/L, the average diameter of as-prepared gold seeds is 5.14 nm, which is suitable for the requirements of subsequent organic microspheres coating. And the surface Zeta potential of gold seeds prepared with 0.1 g/L $HAuCl_4$ is −10.7 mV.

## Properties research of PS@Au photothermal particles

For exploring the morphology of PS microspheres, TEM images were first analyzed and the result is shown in Fig. 1, which exhibits that the microspheres prepared by this method are spherical and the surface is relatively smooth, meanwhile the diameters of

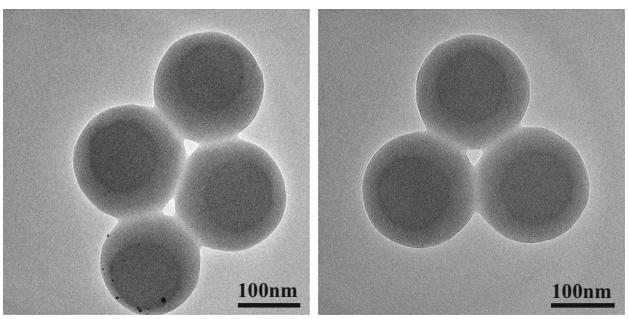


**Figure 1** TEM images of PS microspheres.

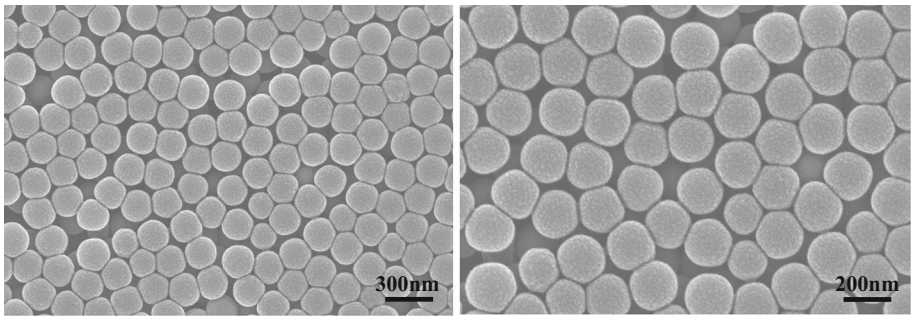


**Figure 2** SEM images of PS microspheres.

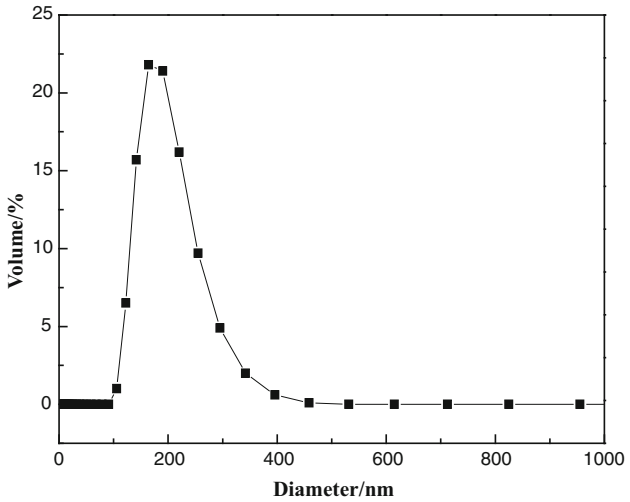


**Figure 3** Particle size distribution curve of PS microspheres.

the microspheres, with an average of 165 nm, are quite uniform.

In order to further study the morphology of PS microspheres, SEM images were characterized and the result is shown in Fig. 2, which indicates that PS microspheres are uniformly dispersed and with good sphericity and smooth surface, which are very suitable for subsequent coating of gold seeds.

Figure 3 shows the particle size distribution curve of PS microspheres, which shows that the particle size distribution exhibits a unimodal pattern with a narrow peak and the average diameter is 164 nm. The result is consistent with the above analysis results of TEM and SEM.

In the process of preparing PS microspheres, the purpose of adding a small amount of AA copolymerized with St is to modify functional groups on the surface of PS microspheres for subsequent adsorption of gold seeds. The microsphere surface was tested to have a negative charge of −31.9 mV. As depicted above, the surface of gold seeds is usually with negative charge. In order to realize electrostatic self-assembly, the microspheres surface should be modified with positive charge and PAH is chosen to modify their surface.

**Table 2** Surface potential of PS microspheres modified with different PAH concentrations

| No | PAH concentration (g/L) | Surface Zeta potential value of PS microspheres before modification (mV) | Surface Zeta potential value of PS microspheres after modification (mV) |
|---|---|---|---|
| 1 | 1.5 | −31.9 | +28.1 |
| 2 | 3.0 | | +38.3 |
| 3 | 4.5 | | +27.8 |

Table 2 shows the surface potential of PS microspheres modified with different PAH concentrations, from which it can be seen that, modified by PAH, the surface potential of PS microspheres turns negative into positive and its value first increases and then decreases with the PAH concentration increasing. When the PAH concentration is 3.0 g/L, the surface potential of modified PS microspheres reaches a positive maximum of +38.3 mV.

The possible reason is that the PAH adsorption capacity and potential on the surface of PS microspheres increase with the increase in PAH concentration when it is low. When PAH concentration reaches a certain value, increasing PAH concentration continuously causes seriously mutual exclusion between PAH molecules, which prevents its adsorption on the surface of PS microspheres so that the surface positive potential of modified PS microspheres decreases.

PS@Au composite particles were prepared via electrostatic self-assembly. The important factors affecting gold content of composite particles surface are potential value of PS microspheres surface and subsequent gold seeds growing times. In order to

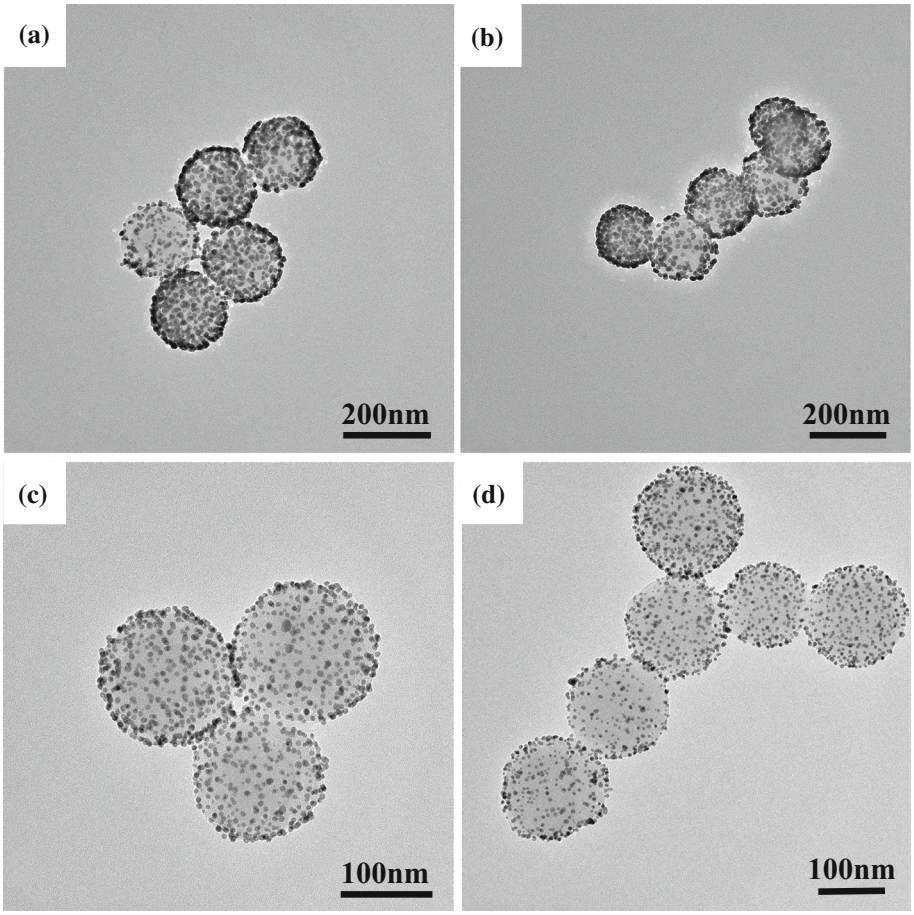


**Figure 4** TEM images of PS@Au composite particles prepared with different surface charge on PS microspheres. **a**, **b** +38.3 mV; **c**, **d** +27.8 mV.

prepare PS@Au composite particles with excellent properties, these two factors were studied in details.

With the amount of gold seeds unchangeable, modified PS microspheres with surface potential of +38.3 and +27.8 mV were chosen, respectively, to prepare composite particles. Figure 4 shows that both of two kinds of PS microspheres with different surface potential adsorb gold seeds on the surface, forming the morphology of composite particles coated by gold seeds. Comparing the two kinds of composite particles with different surface potentials, it is found that the adsorption capacity of gold seeds of PS microspheres surface with higher potential is more than that with lower potential. This is because gold seeds are attached to PS microspheres surface by electrostatic adsorption. For PS microspheres with the same diameter, the higher the surface charge density is, the more the adsorption capacity of gold seeds is, so the coating effect becomes much better. It can be concluded that the coating effect of PS microspheres gets better with the increase in PS microspheres surface charge density. So improving the surface charge density of PS microspheres effectively is a prerequisite for the formation of dense coating.

The PS@Au composite particles were characterized by XRD, and the result is shown in Fig. 5. It can be seen that the composite particles show four strong diffraction peaks. Compared with gold XRD standard card (JCPDS 04-0784), it is confirmed that the composite particles contain gold.

Figure 4 also shows that PS@Au composite particles do not form dense gold nanoshells after gold seeds being adsorbed on the surface of PS microspheres, so further gold seeds growth is needed. Adding reducing agent into chloroauric acid solution directly to prepare gold seeds is a homogeneous nucleation process. According to laws of thermodynamics, the free energy of this system ($\Delta G_V$) will decrease due to generation of solid phase in this process, but continuous formation of solid–liquid interface will increase the surface energy ($\Delta G_S$) of solid interface. In the stage of nucleation, the diameter of crystal nuclei is very small and the total

energy of the system increases ($\Delta G_S > \Delta G_V$), so homogeneous nucleation is not a spontaneous process. For chloroauric acid solution, different reducing agents need different energy of homogeneous nucleation, and the stronger reducing power is, the easier homogeneous nucleation is. However, the heterogeneous nucleation will occur if there are some seeds that have the same crystal structure as substance to be crystallized in the system. At this time, the nucleation energy ($\Delta G_C$) is close to zero and crystallization can be approximated as a spontaneous process. Thus, gold produced by the reduction of chloroauric acid can grow on the surface of gold seeds spontaneously after adding gold seeds, without a secondary homogenous nucleation process.

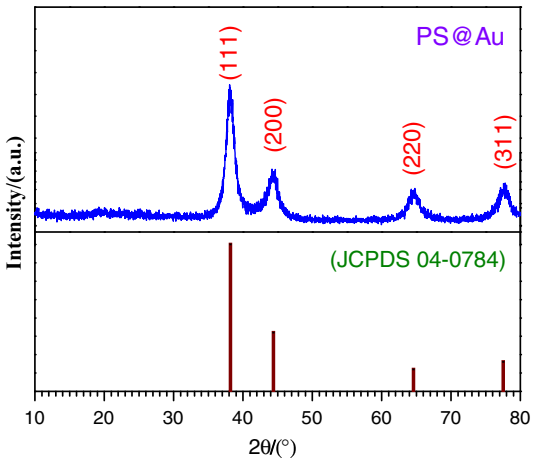


**Figure 5** XRD of PS@Au composite particles.

According to the above theory, to ensure that gold reduced subsequently grows on the surface of gold seeds, hydroxylamine hydrochloride, with weaker reducing capacity than sodium borohydride, was chosen as a reducing agent, lowering the possibility of the secondary homogenous nucleation. Meanwhile, to decrease the secondary nucleation caused by high chloroauric acid concentration, chloroauric acid was added repeatedly to keep gold seeds growing. Figure 6 shows TEM images of the morphology of PS@Au composite particles prepared with different gold seeds growing times, illustrating that,

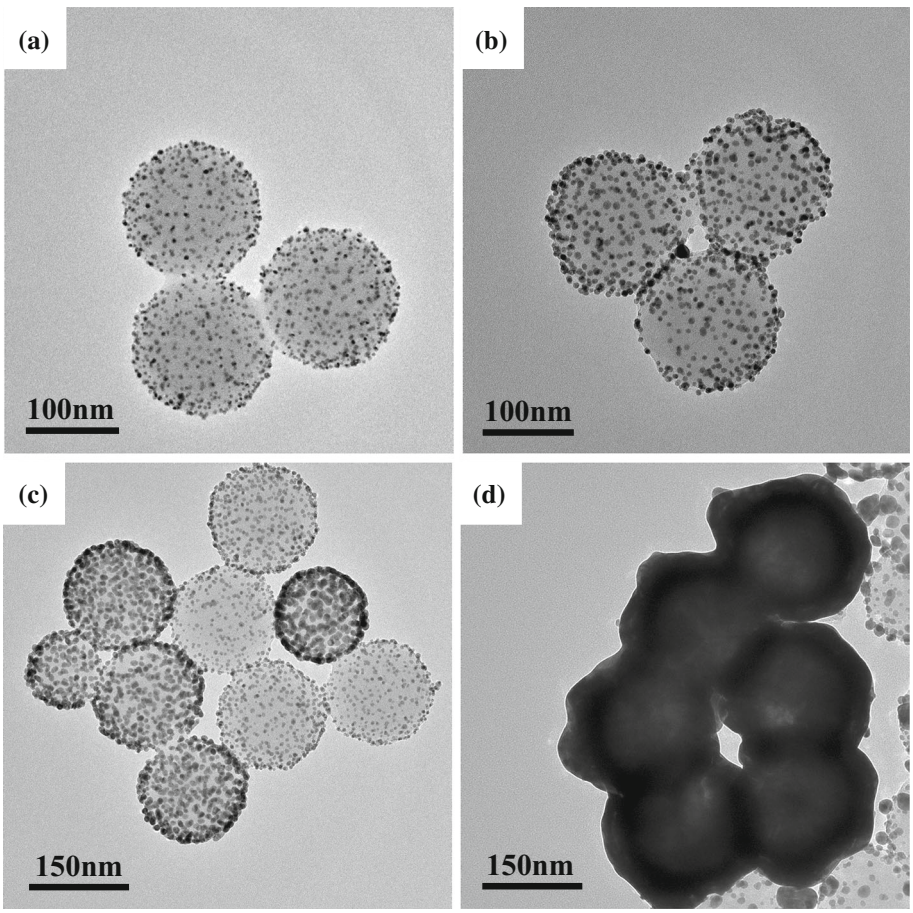


**Figure 6** TEM images of PS@Au composite particles with different gold seeds growing times. **a** PS microspheres adsorbed gold seeds; **b** two times; **c** three times; **d** four times.

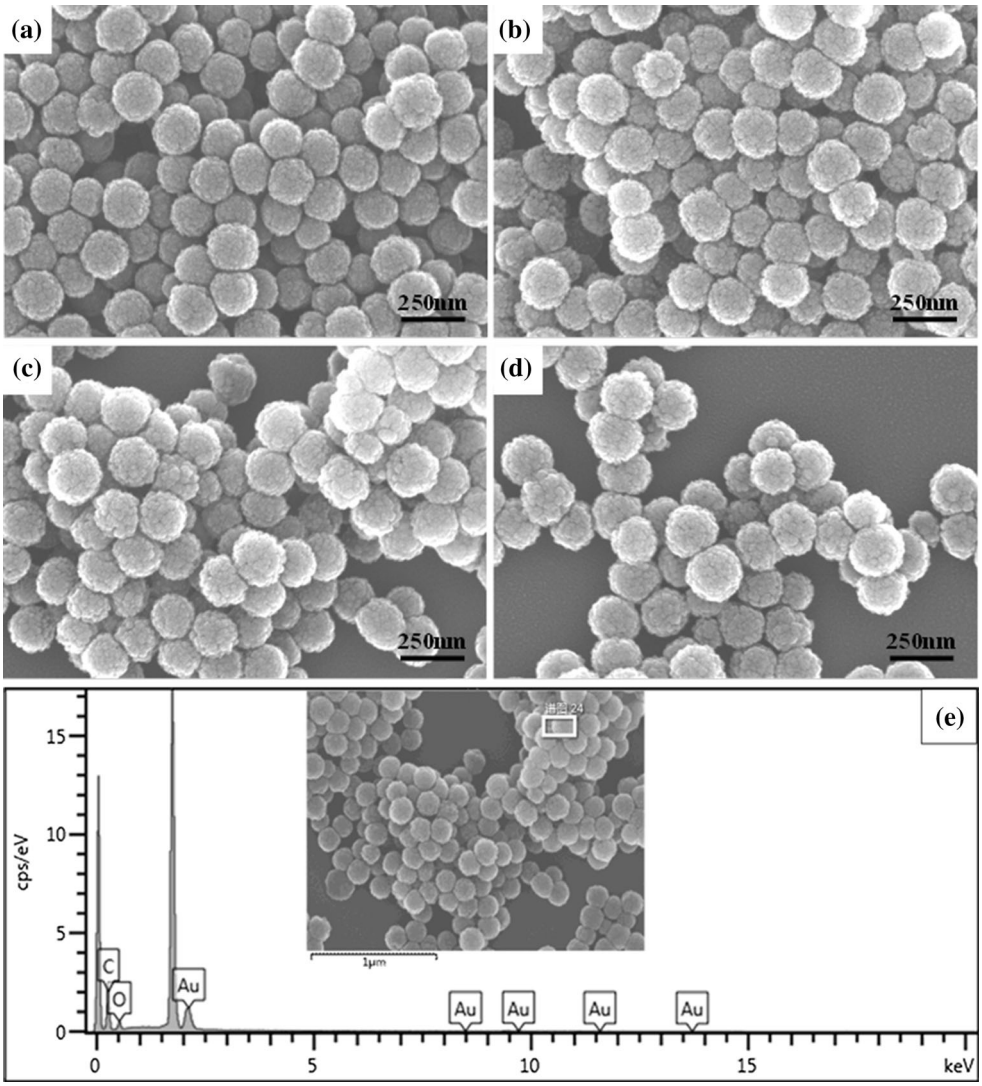


**Figure 7** SEM images of PS@Au composite particles with different gold seeds growing times and EDS. **a** PS microspheres adsorbed gold seeds; **b** two times; **c** three times; **d** four times; **e** EDS.

with the increase in gold seeds growing times, the diameter of gold particles on the surface of PS microspheres increases gradually, leading to a tendency for the formation of a gold nanoshell. When gold seeds have grown for four times, most PS microspheres form dense structure coated with gold on the surface, achieving the desired objectives.

To further study the surface morphology of PS@Au composite particles with different gold seeds growth times, SEM and EDS were characterized and the results are shown in Fig. 7. It can be seen that the diameter of gold particles on the surface of PS microspheres is increasing and there is a trend of forming a gold nanoshell with the increase in gold seeds growing times (Fig. 7a–d). When gold seeds

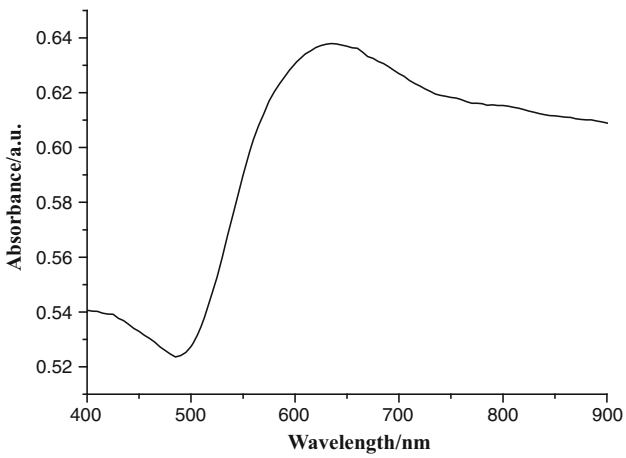


**Figure 8** UV–Vis spectrum of PS@Au composite particles.

have grown for four times, most PS microspheres form dense structure coated with gold on the surface, achieving the desired objectives, which is consistent with the results of TEM images. To further verify that the surface particles were gold nanoparticles, EDS was characterized and the result is shown in Fig. 7e, which illustrates that PS@Au composite particles contain gold element and the content is 19.52% (w.t.%).

## Photothermal properties study of PS@Au composite particles

In order to study the photothermal properties of PS@Au composite particles, UV–Vis spectrum was firstly characterized (Fig. 8), which shows that the maximum absorption peak of the PS@Au composite particles redshifts to 635 nm, comparing with the peak of gold nanoparticles at 520 nm [1]. As the increase in the wavelength, the absorbance decreases slowly in the range of 700–900 nm, which confirms that the composite particles have NIR absorption. Then, these particles were dispersed into water and the temperature variation of different irradiation time was tested and compared to pure water, which was irradiated with a NIR light source with a center wavelength of 808 nm and output power of 0.97 W. The results are shown in Table 3 and Fig. 9. It is shown that the elevated temperature of PS@Au composite particles with fewer gold seeds growth times is not obvious, almost as same as pure water. However, the temperature of PS@Au composite particles with four gold seeds growing times reaches 38 °C as it goes up for 5 min. The reason is that gold particles are at dispersed state on the surface of PS microspheres, and the surface plasmon resonance absorption of each gold particle is mainly at 530 nm when gold seeds grow for fewer times, so little heat generates when irradiated with NIR light. With the increase in gold seeds growing times, gold particles begin to connect each other and gradually form a shell structure, whose surface plasmon resonance absorption redshifts, therefore resulting in photothermal properties in the NIR region.

Through the above research and analysis, PS@Au composite particles, with core–shell structures and photothermal properties in the NIR region, were prepared successfully via electrostatic self-assembly method, and the preliminary purposes were achieved.

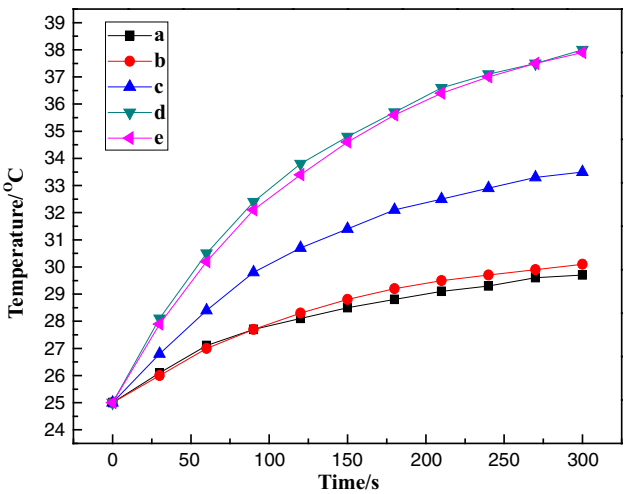


**Figure 9** Photothermal properties curves of water and PS@Au composite particles with different gold seeds growing times. **a** pure water; **b** one time; **c** two times; **d** three times; **e** four times.

**Table 3** Photothermal data of water and PS@Au composite particles with different gold seeds growing times

| Sample name | Initial temperature (°C) | Temperature of the system after 5-min irradiation (°C) | The elevated temperature of the system (°C) |
|---|---|---|---|
| Pure water | 25.0 | 29.7 | 4.7 |
| PS@Au composite particles growing one time | 25.0 | 30.1 | 5.1 |
| PS@Au composite particles growing two times | 25.0 | 33.5 | 8.5 |
| PS@Au composite particles growing three times | 25.0 | 37.9 | 12.9 |
| PS@Au composite particles growing four times | 25.0 | 38.0 | 13.0 |

## Conclusions

PS@Au composite particles with good photothermal effect were prepared successfully. Firstly, PS microspheres, with negative charge on their surface, were synthesized by emulsifier-free emulsion polymerization, whose surface Zeta potential turned into +38.3 mV after modified with PAH. Secondly, gold seeds were prepared via sodium borohydride reducing chloroauric acid. It is confirmed that they have small particle size and negative charge on the surface. Then, through electrostatic self-assembly, gold seeds were easily adsorbed on the surface of PS microspheres modified with PAH. When gold seeds have grown for four times, PS@Au composite particles, coated with gold nanoshells, were obtained. Finally, photothermal properties study shows that PS@Au composite particles have good photothermal effect and can be used as photothermal particles in cancer PTT.

## Acknowledgement

The authors are grateful for the financial support provided by the National Natural Science Foundation of Shaanxi (No. 2015JM2050), Key Project of Shanghai Space Foundation (No. SAST2016051) and National Undergraduate Training Programs for Innovation (No. 201610699269).

## References

[1] Cheng L, Wang C, Feng L, Yang K, Liu Z (2014) Functional nanomaterials for phototherapies of cancer. Chem Rev 114:10869–10939

[2] Johannsen M, Gneveckow U, Thiesen B, Taymoorian K, Cho CH, Waldöfner N, Scholz R, Jordan A, Loening SA, Wust P (2007) Thermotherapy of prostate cancer using magnetic nanoparticles: feasibility, imaging, and three-dimensional temperature distribution. Eur Urol 52:1653–1662

[3] Soenen SJ, Parak WJ, Rejman J, Manshian B (2015) (Intra) cellular stability of inorganic nanoparticles: effects on cytotoxicity, particle functionality, and biomedical applications. Chem Rev 115:2109–2135

[4] Bucharskaya A, Maslyakova G, Dikht N, Navolokin N, Terentyuk G, Bashkatov A, Genina E, Tuchin V, Khlebtsov B, Khlebtsov N (2016) Cancer cell damage at laser-induced plasmon-resonant photothermal treatment of transplanted liver tumor. BioNanoScience 6:256–260

[5] Zhang B, Zhang H, Tian L, Li X, Li W, Fan X, Ali N, Zhang Q (2015) Magnetic microcapsules with inner asymmetric structure: controlled preparation, mechanism, and application to drug release. Chem Eng J 275:235–244

[6] Zhang B, Zhang H, Fan X, Li X, Yin D, Zhang Q (2013) Preparation of thermoresponsive $Fe_3O_4$/P (acrylic acid–methyl methacrylate–N-isopropylacrylamide) magnetic composite microspheres with controlled shell thickness and its releasing property for phenolphthalein. J Colloid Interface Sci 398:51–58

[7] Hauck TS, Jennings TL, Yatsenko T, Kumaradas JC, Chan WC (2008) Enhancing the toxicity of cancer chemotherapeutics with gold nanorod hyperthermia. Adv Mater 20:3832–3838

[8] Park JH, von Maltzahn G, Ong LL, Centrone A, Hatton TA, Ruoslahti E, Bhatia SN, Sailor MJ (2010) Cooperative nanoparticles for tumor detection and photothermally triggered drug delivery. Adv Mater 22:880–885

[9] Xiao Z, Ji C, Shi J, Pridgen EM, Frieder J, Wu J, Farokhzad OC (2012) DNA self-assembly of targeted near-infrared-responsive gold nanoparticles for cancer thermo-chemotherapy. Angew Chem 124:12023–12027

[10] You J, Zhang G, Li C (2010) Exceptionally high payload of doxorubicin in hollow gold nanospheres for near-infrared light-triggered drug release. ACS Nano 4:1033–1041

[11] Liu H, Liu T, Wu X, Li L, Tan L, Chen D, Tang F (2012) Targeting gold nanoshells on silica nanorattles: a drug cocktail to fight breast tumors via a single irradiation with near-infrared laser light. Adv Mater 24:755–761

[12] Liu T, Chao Y, Gao M, Liang C, Chen Q, Song G, Cheng L, Liu Z (2016) Ultra-small $MoS_2$ nanodots with rapid body clearance for photothermal cancer therapy. Nano Res 9:3003–3017

[13] Chen M, Chen S, He C, Mo S, Wang X, Liu G, Zheng N (2016) Safety profile of two-dimensional Pd nanosheets for photothermal therapy and photoacoustic imaging. Nano Res. doi:10.1007/s12274-016-1349-6

[14] Feng B, Zhou F, Wang D, Xu Z, Yu H, Li Y (2016) Gold nanomaterials for treatment of metastatic cancer. Sci China Chem 59:984–990

[15] Nikoobakht B, El-Sayed MA (2003) Preparation and growth mechanism of gold nanorods (NRs) using seed-mediated growth method. Chem Mater 15:1957–1962

[16] Shanmugam V, Selvakumar S, Yeh C-S (2014) Near-infrared light-responsive nanomaterials in cancer therapeutics. Chem Soc Rev 43:6254–6287

[17] Ke H, Wang J, Dai Z, Jin Y, Qu E, Xing Z, Guo C, Yue X, Liu J (2011) Gold-nanoshelled microcapsules: a theranostic agent for ultrasound contrast imaging and photothermal therapy. Angew Chem 123:3073–3077

[18] Skrabalak SE, Chen J, Au L, Lu X, Li X, Xia Y (2007) Gold nanocages for biomedical applications. Adv Mater 19:3177–3184

[19] Wang Y, Xie X, Wang X, Ku G, Gill KL, O'Neal DP, Stoica G, Wang LV (2004) Photoacoustic tomography of a nanoshell contrast agent in the in vivo rat brain. Nano Lett 4:1689–1692

[20] Jiménez-Pérez J, Gamboa GL, Fuentes RG, Ramírez JS, Pacheco ZC, López-y-López V, Tepech-Carrillo L (2016) Synthesis and thermal properties of new bionanofluids containing gold nanoparticles. Appl Phys A 122:925

[21] Yi X, Chen L, Zhong X, Gao R, Qian Y, Wu F, Song G, Chai Z, Liu Z, Yang K (2016) Core–shell Au@$MnO_2$ nanoparticles for enhanced radiotherapy via improving the tumor oxygenation. Nano Res 9:3267–3278

[22] Kim HS, Lee DY (2017) Photothermal therapy with gold nanoparticles as an anticancer medication. J Pharm Investig 47:19–26

[23] Ghosh S, Dutta S, Gomes E, Carroll D, D'Agostino R Jr, Olson J, Guthold M, Gmeiner WH (2009) Increased heating efficiency and selective thermal ablation of malignant tissue with DNA-encased multiwalled carbon nanotubes. ACS Nano 3:2667–2673

[24] Burke A, Ding X, Singh R, Kraft RA, Levi-Polyachenko N, Rylander MN, Szot C, Buchanan C, Whitney J, Fisher J (2009) Long-term survival following a single treatment of kidney tumors with multiwalled carbon nanotubes and near-infrared radiation. Proc Natl Acad Sci 106:12897–12902

[25] Wang X, Wang C, Cheng L, Lee S-T, Liu Z (2012) Noble metal coated single-walled carbon nanotubes for applications in surface enhanced Raman scattering imaging and photothermal therapy. J Am Chem Soc 134:7414–7422

[26] Gangadharaiah S, Farid A, Mishchenko E (2008) Charge response function and a novel plasmon mode in graphene. Phys Rev Lett 100:166802

[27] Yang K, Zhang S, Zhang G, Sun X, Lee S-T, Liu Z (2010) Graphene in mice: ultrahigh in vivo tumor uptake and efficient photothermal therapy. Nano Lett 10:3318–3323

[28] Robinson JT, Tabakman SM, Liang Y, Wang H, Sanchez Casalongue H, Vinh D, Dai H (2011) Ultrasmall reduced graphene oxide with high near-infrared absorbance for photothermal therapy. J Am Chem Soc 133:6825–6831

[29] Wang Y, Wang K, Zhao J, Liu X, Bu J, Yan X, Huang R (2013) Multifunctional mesoporous silica-coated graphene nanosheet used for chemo-photothermal synergistic targeted therapy of glioma. J Am Chem Soc 135:4799–4804

[30] Tian Q, Tang M, Sun Y, Zou R, Chen Z, Zhu M, Yang S, Wang J, Wang J, Hu J (2011) Hydrophilic flower-like CuS superstructures as an efficient 980 nm laser-driven photothermal agent for ablation of cancer cells. Adv Mater 23:3542–3547

[31] Goel S, Chen F, Cai W (2014) Synthesis and biomedical applications of copper sulfide nanoparticles: from sensors to theranostics. Small 10:631–645

[32] Brown KR, Natan MJ (1998) Hydroxylamine seeding of colloidal Au nanoparticles in solution and on surfaces. Langmuir 14:726–728

[33] Brown KR, Walter DG, Natan MJ (2000) Seeding of colloidal Au nanoparticle solutions. 2. Improved control of particle size and shape. Chem Mater 12:306–313

[34] Brown KR, Lyon LA, Fox AP, Reiss BD, Natan MJ (2000) Hydroxylamine seeding of colloidal Au nanoparticles. 3. Controlled formation of conductive Au films. Chem Mater 12:314–323